

Strength, toughness and R-curve behaviour of SiC whisker-reinforced composite Si₃N₄ with reference to monolithic Si₃N₄

S. R. CHOI*[‡], J. A. SALEM[‡]

*Cleveland State University, Cleveland, OH 44115, USA and [‡]NASA Lewis Research Center, Cleveland, OH 44135, USA

The flexural strength and fracture toughness of 30 vol% SiC whisker-reinforced Si₃N₄ material were determined as a function of temperature from 25 to 1400 °C in an air environment. It was found that both strength and toughness of the composite material were almost the same as those of the monolithic counterpart. The room-temperature strength was retained up to 1100 °C; however, appreciable strength degradation started at 1200 °C and reached a maximum at 1400 °C due to stable crack growth. In contrast, the fracture toughness of the two materials was independent of temperature with an average value of 5.66 MPa m^{1/2}. It was also observed that the composite material exhibited no rising R-curve behaviour at room temperature, as was the case for the monolithic material. These results indicate that SiC whisker addition to the Si₃N₄ matrix did not provide any favourable effects on strength, toughness and R-curve behaviour.

1. Introduction

Ceramics have attracted particular interest for high-temperature structural applications in advanced heat engines and heat recovery systems. The major limitation for assuring the reliability of the ceramic materials is their low fracture toughness. The composite approach, in which a low-modulus and low-strength matrix material is reinforced via the incorporation of strong and high-modulus SiC whiskers, has shown to be one of the alternatives to improve toughness and strength. Alumina composites reinforced with SiC whiskers have exhibited excellent mechanical properties compared to their matrix base materials: toughness, strength, and fatigue and thermal shock resistance are substantially higher for the composite materials [1–6]. Major mechanisms responsible for these superior properties are believed to be crack deflection, whisker pull-out and/or whisker bridging [1, 7–10].

On the other hand, the composite approach to Si₃N₄ via SiC whiskers has shown limited success, depending on the fabrication process. It has been demonstrated that the fracture toughness is increased significantly (20–30%) by the addition of 20–30 vol% SiC whiskers but that the corresponding strength is not significantly improved, or in some cases, is even worse than for the monolithic materials [10–14]. In addition, the resistance of the composite to impact/erosion, creep and cyclic crack growth has also exhibited a varying degree of improvement or deterioration [15–20]. The increased processing complexity of composites may be the major cause of such problems.

The purpose of this study is to better understand the strength and toughness behaviour of 30 vol% SiC whisker-reinforced Si₃N₄ material. For this purpose, strength and toughness were measured as a function of temperature from 25 to 1400 °C in air. The indentation strength was also examined at room temperature to determine R-curve behaviour. Similar monolithic Si₃N₄ material was utilized to provide a baseline of comparison.

2. Experimental procedure

The materials used in this study were based on Garrett GN-10 composite and monolithic Si₃N₄ (Garrett Ceramic Components, Allied Signal, Torrance, California). The material fabrication has been described elsewhere [14]. Briefly, Si₃N₄ powder composition was slip-cast into 50 mm diameter, 75 mm height billets, glass-encapsulated by the ASEA method (ABB Autoclave Systems, Columbus, Ohio) and hot-isostatically pressed to produce monolithic Si₃N₄ material. Part of the same powder batch was blended with 30 vol% SiC whiskers by ACMC (Advanced Composite Materials Corp., Greer, South Carolina) and processed with the same procedures as the monolithic. Densities of the composite and monolithic materials were 3.27 and 3.31 g cm⁻³, respectively.

The billets of both composite and monolithic materials were cut to produce the flexure test specimens such that the prospective tensile surfaces of the specimens were normal to the hot pressing direction. As-received strength was determined from the flexure specimens (2.7 mm × 4 mm × 50 mm) with a four-point

bend fixture with 20/40 mm spans as a function of temperature from 25 to 1400 °C in an air environment. The crosshead speed employed was 0.2 mm min⁻¹. The number of test specimens per temperature was three to ten.

The chevron-notch method was used to evaluate fracture toughness at temperatures from 25 to 1400 °C. Three to six chevron-notch bend specimens measuring 3 mm by 5.6 mm in thickness and height, respectively, were tested at each temperature using a four-point flexure fixture with spans of 20 and 40 mm. A slow stroke rate of 0.01 mm min⁻¹ was utilized to ensure stable crack extension during testing. The fracture toughness was calculated based on the analysis by Munz *et al.* [21]. In addition, toughness measurements by the single-edge precracked beam (SEPB) [22] and indentation strength [23] methods were also made at room temperature to see if there exists a difference in toughness values between the test methods.

Room-temperature R-curve behaviour was estimated using the indentation strength technique proposed by Krause [24]. The test specimens were 3 mm × 5.6 mm × 25 mm MOR bars, and the centre of the polished prospective tensile surface of each specimen was indented with a Vickers microhardness indenter over a load range of 49 to 294 N. The subsequent strength tests for the indented samples were conducted using a four-point bend fixture with 10/18 mm spans at a crosshead speed of 0.2 mm min⁻¹ in room temperature air. Three to four specimens were tested at each indentation load.

3. Results and discussion

3.1. Strength

Fig. 1 gives the results of the as-received strength measurements for the composite and monolithic

materials, where fracture strength is plotted as a function of test temperature. The room-temperature strength was found to be $\sigma_f = 698 \pm 85$ MPa and 732 ± 61 MPa for the composite and monolithic materials, respectively. Weibull modulus in the strength distribution was not available in this study due to the limited number of test specimens (typically less than ten). However, the Weibull modulus (τ) can be estimated approximately using a formula of $\tau \approx 1.2/(C_V)$ as proposed by Ritter *et al.* [25], where C_V is the coefficient of variation of the mean strength. Using this relation together with the obtained values of C_V for the two materials at room temperature, Weibull moduli of the composite and monolithic are estimated to be $\tau = 9.8$ and 14.4, respectively. Despite the insufficient number of test specimens for the reliable evaluation of Weibull parameters, the estimated Weibull modulus is in good agreement with the typical range of $\tau \approx 7$ to 15 commonly observed for sintered Si₃N₄ materials. It is important to note that a low Weibull modulus suggests non-uniformity and/or inhomogeneity in composition and microstructure for the materials.

Examination of the fracture surfaces for both materials showed that most of failures originated from surface and sub-surface porous regions, coarse-grained regions, and agglomerates [14]. Typical examples of such porous region- and agglomerate-associated failures are shown in Fig. 2. The agglomerate found in Fig. 2c was identified as a chunk of nitride, but not associated with processing contaminants such as glass and metallic particles (e.g. iron).

For both materials, the room-temperature strength was retained with little variation up to 1100 °C; however, appreciable strength degradation occurred from 1200 °C and reached a maximum at 1400 °C. The maximum strength degradation at 1400 °C, relative to

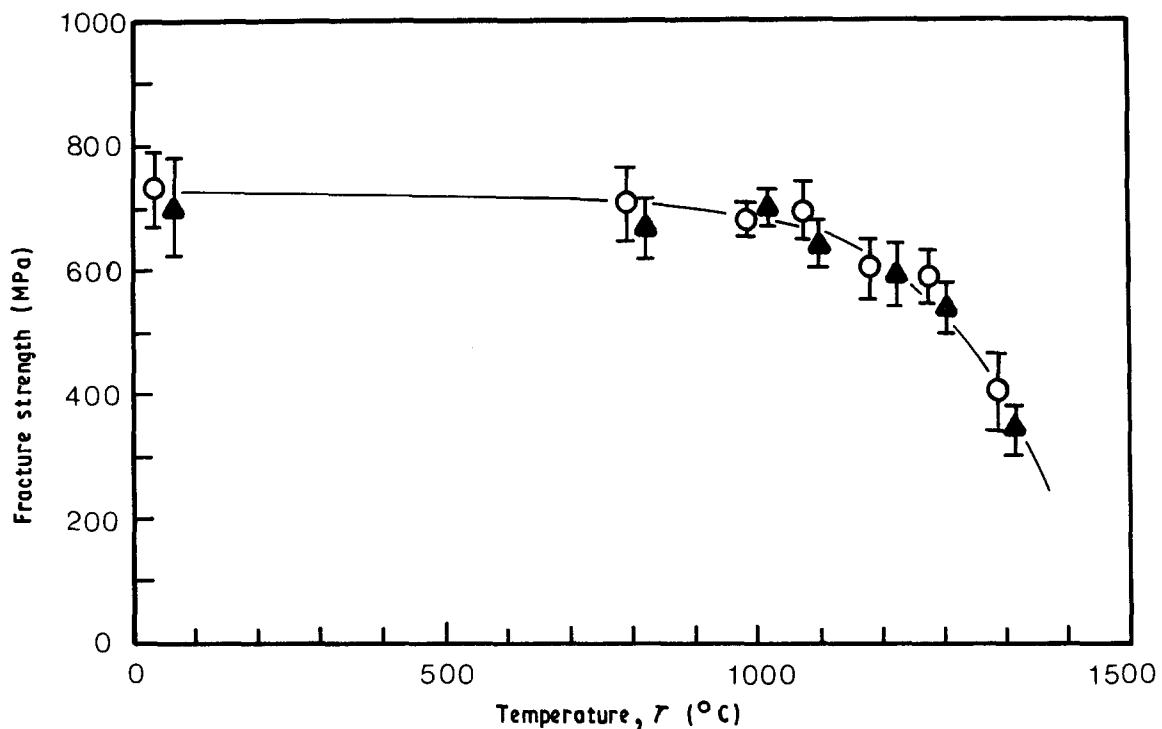


Figure 1 As-received strength of (▲) SiC whisker-reinforced Si₃N₄ and (○) monolithic Si₃N₄ as a function of temperature in air. Error bar indicates ± 1.0 standard deviation.

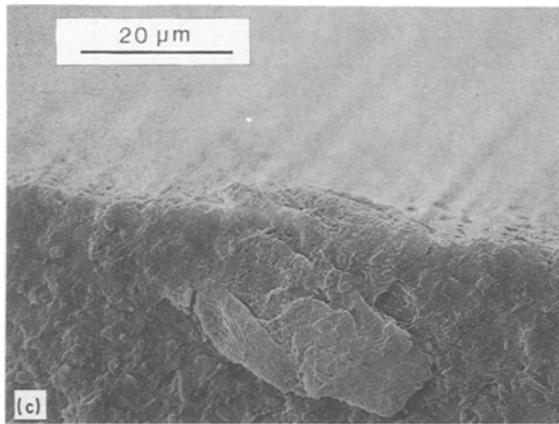
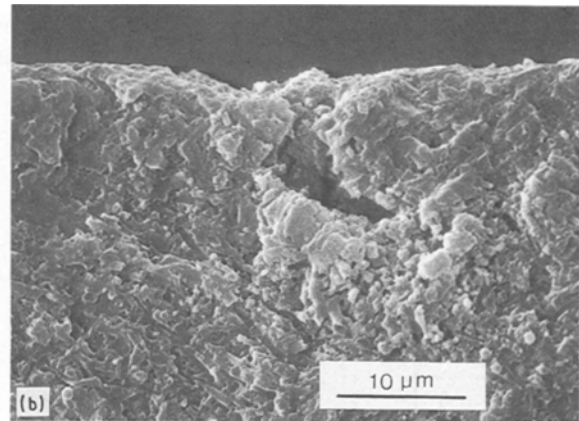
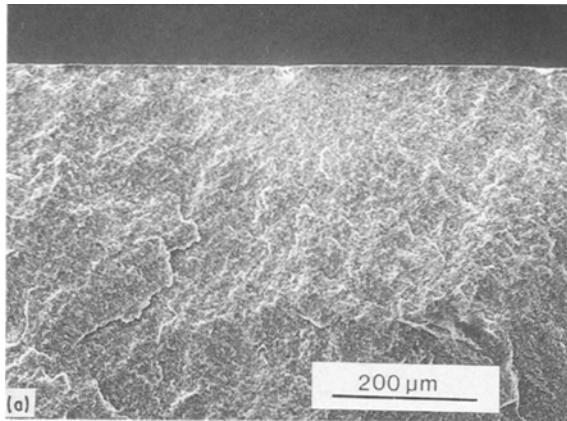


Figure 2 SEM fractographs: (a) overall view showing fracture origin and fracture mirror for composite specimen failed at $\sigma_f = 706$ MPa at 800°C ; (b) magnified view of (a) revealing fracture origin as porous region; (c) agglomerate-associated failure in monolithic specimen failed at $\sigma_f = 699$ MPa at 25°C .

mental error, it can be concluded that the strengths of both composite and monolithic materials are virtually the same, as seen in Fig. 1. This indicates that whisker addition to the Si_3N_4 matrix did not provide any favourable effect on strength, consistent with earlier work [10, 13].

the room-temperature strength, reached 50 and 45% for the composite and monolithic materials, respectively. This high-temperature strength degradation, particularly at 1400°C , is believed to be associated with slow crack growth and creep deformation due to the softening of the crystallized grain boundaries. A large region of such slow crack growth occurring at 1400°C for the composite material is shown in Fig. 3. Also note the appearance of extensive glassy phases that occurred, probably due to oxidation.

In general, the strength of the monolithic material was about 5 to 15% higher compared to that of the composite. However, in view of the range of experi-

3.2. Fracture toughness

The results of the fracture toughness measurements from the chevron-notch method are presented in Fig. 4. Here the measured fracture toughness for both materials is plotted against test temperature from 25 to 1200°C . Contrary to the case found in the strength behaviour, toughness degradation with increasing temperature was not observed for the two materials. Over the test temperature range, the room-temperature toughness ($K_{IC} = 5.46 \pm 0.28$ and 5.32 ± 0.30 $\text{MPa m}^{1/2}$ for the composite and monolithic, respectively) remained almost unchanged within $\leq 10\%$, indicating that toughness for both materials is independent of test temperature up to 1200°C . Also note the negligibly small difference in toughness values

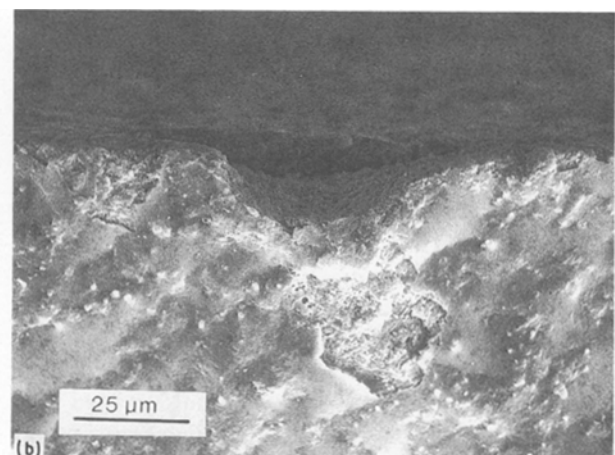
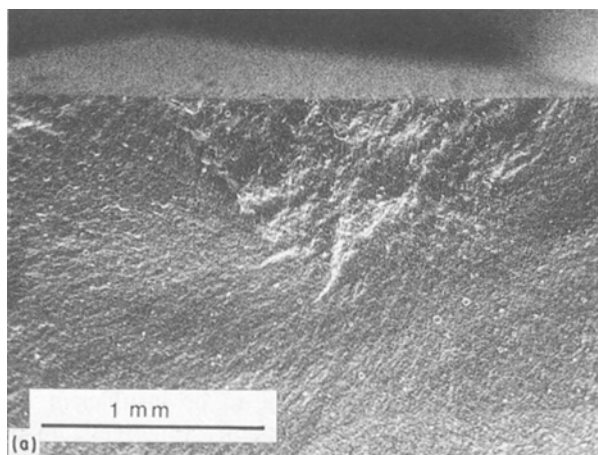


Figure 3 SEM fractographs of composite specimen failed at $\sigma_f = 329$ MPa at 1400°C : (a) overall view showing a large region of slow crack growth; (b) magnified view of (a) in slow crack growth region showing glassy phases extensively covering the fracture surface.

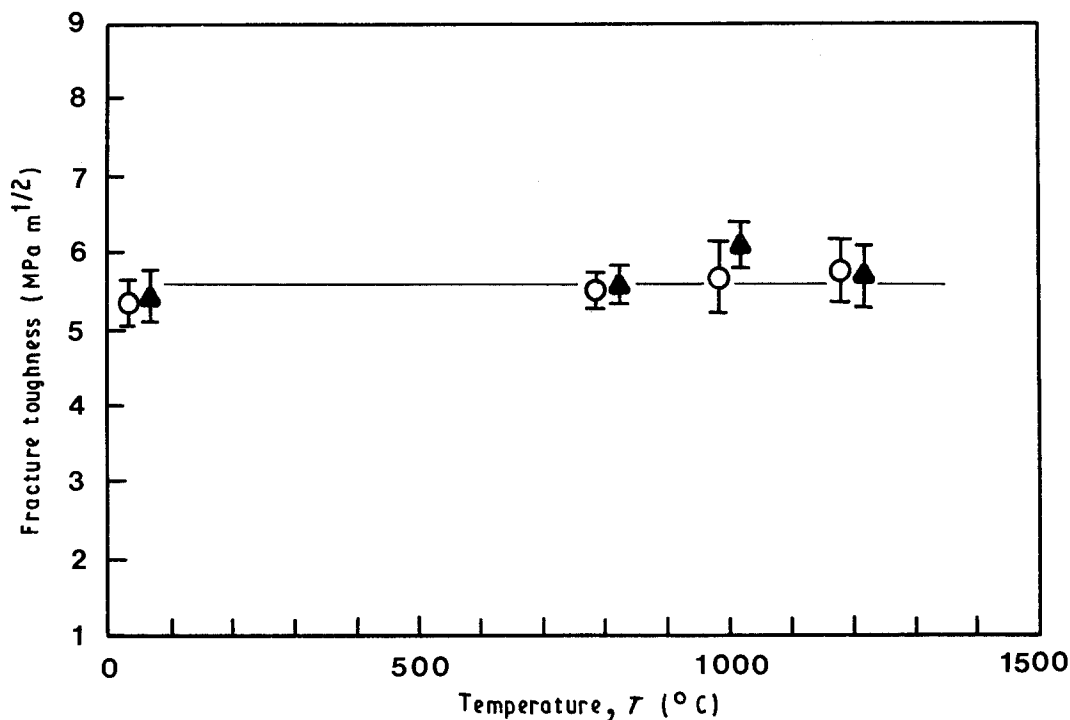


Figure 4 Fracture toughness of (▲) composite and (○) monolithic materials as a function of temperature in air. The horizontal line represents an average value of toughness ($= 5.66 \text{ MPa m}^{1/2}$) for all data. Error bar indicates ± 1.0 standard deviation.

between the two materials. The overall fracture toughness was found to be $K_{IC} = 5.66 \pm 0.26 \text{ MPa m}^{1/2}$, as indicated as a horizontal line in Fig. 4.

It should be noted that, although not presented in Fig. 4, an unusually high fracture toughness of $K_{IC} \geq 10 \text{ MPa m}^{1/2}$ was obtained for both materials at the temperature of 1400°C . This is due to increased plasticity and/or creep deformation associated with the combined effects of high temperature and the slow testing speed of 0.01 mm min^{-1} , as reported previously [14]. Thus, the chevron-notch method may be inappropriate for such high temperatures. The SEPB method in an inert environment, however, is thought to be a good alternative to measure fracture toughness at that high temperature [26].

A summary of the fracture toughness evaluated at room temperature from the chevron notch (CN), SEPB, and indentation strength (IS) methods is shown in Fig. 5. It can be seen here that the fracture toughness thus obtained was not dependent on the test method for both materials. Also note that there was virtually no difference in fracture toughness between the two materials. The overall fracture toughness was found to be $K_{IC} = 5.41 \pm 0.20 \text{ MPa m}^{1/2}$, as shown in Fig. 5. This result implies that crack growth resistance of the materials remains constant regardless of the crack size, which is either in the micro-crack (indented) or the macro-crack (SEPB and CN) regime. Crack growth resistance as a function of crack size, called R-curve behaviour, will be discussed below.

The fact that no appreciable difference in fracture toughness between the two materials existed (see Figs 4 and 5) implies that the toughening contribution from whisker addition was ineffective for the current composite material system. This contrasts with the result of the previous study on 30 vol % SiC

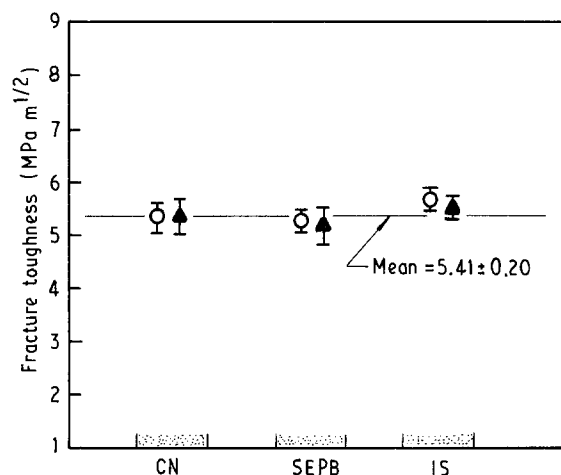


Figure 5 Room-temperature fracture toughness of (▲) composite and (○) monolithic materials evaluated from three different techniques of chevron-notch (CN), single-edge precracked beam (SEPB) and indentation strength (IS) methods. A mean value of $5.41 \text{ MPa m}^{1/2}$ was obtained for all data. Error bar indicates ± 1.0 standard deviation.

whisker-Si₃N₄ composite where about 30% increase in fracture toughness was achieved at room temperature [26]. Toughening mechanisms such as crack deflection by the whiskers and both whisker bridging and whisker pull-out have been suggested and observed to be operative for whisker-reinforced ceramics [1, 7–10]. Fracture surfaces of the composite material exhibited whisker pull-out and whisker impressions to some extent (Fig. 6). However, the number and extent of fibre pull-outs are thought to be insufficient to achieve a reasonably high fracture toughness. Also note that many fibres were aligned to the direction parallel to the fracture plane, as observed from the orientation of the fibre impressions in Fig. 6b. It

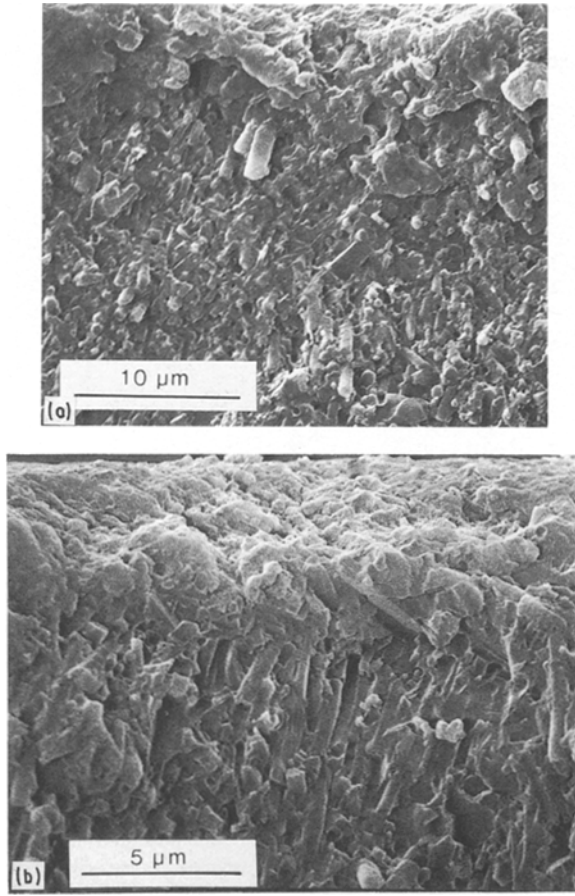


Figure 6 Fracture surfaces of composite material showing (a) whisker pull-out and (b) orientation of whisker impressions which is parallel to the fracture surface.

should be noted that proper alignment of whiskers relative to the crack plane (i.e. whisker axis aligned perpendicular to crack plane) is a prerequisite to enhance fracture toughness of the composite material.

Recently, Becher *et al.* [8] made an attempt to model the toughening behaviour of whisker-reinforced ceramics based on both the stress intensity and the energy change introduced by bridging whiskers with some simplifying assumptions. Their resulting expression for the toughening contribution (δK) is

$$\delta K = \frac{1}{2}[(K_0^2 + Q)^{1/2} - K_0] \quad (1)$$

where

$$Q = \frac{2(\sigma_f^w)^2 V_f E^c G^m r}{3(1 - \mu^2) E^w G^i}$$

and where K_0 is the matrix toughness, σ_f^w the whisker strength, V_f the volume fraction of whiskers, μ the Poisson's ratio of the composite, r the whisker ratio and E and G are the Young's modulus and fracture energy, respectively. The superscripts c, w, m, and i denote composite, whisker, matrix and interface, respectively. For the given whisker (strength, E and V_f) and given matrix (toughness) conditions, the toughening is strongly dependent on the interface fracture energy G^i . In other words, the interfacial fracture energy must be small so that partial debonding of whisker along the whisker-matrix interface occurs to form the whisker bridging. In order to obtain a 10% increase in toughening from the current composite,

the fracture energy ratio of matrix to interface given in Equation 1 needs to be $G^m/G^i \approx 10^{-6}$ for experimental and literature values of $\sigma_f^w \approx 8$ GPa [27], $r = 0.2$ μm , $\mu \approx 0.2$, $E^0 \approx 300$ GPa, $E^w \approx 580$ GPa [27], $K_0 = 5.4$ $\text{MPa m}^{1/2}$ and $\delta K = 0.54$ $\text{MPa m}^{1/2}$ together with $V_f = 0.3$. To achieve a 50% increase in toughening, for example, the ratio G^m/G^i should be increased by factor of 10 from the 10% toughened composite system. Controlling the matrix-whisker interface is thus crucial in tailoring the toughness property of the composite materials. However, complexities involved with interface surface chemistry, whisker morphology and thermal expansion mismatches are known to be inevitable [28].

3.3. R-curve behaviour

Damage or flaw tolerance that results from an increasing resistance to stable crack propagation is a desirable material property for structural ceramics. Krause [24] has shown that such R-curve behaviour could be evaluated from the indentation strength data, assuming that fracture resistance (K_r) is related to the crack length (c) by a power-law relationship. The fracture resistance and the indentation strength (σ_f) relations are expressed by

$$K_r = kc^m \quad (2)$$

$$\sigma_f = \frac{k(3 + 2m)}{4\beta} \left(\frac{4P\Gamma}{k(1 - 2m)} \right)^{(2m-1)/(2m+3)} \quad (3)$$

where k and m are constants, Γ and β are the dimensionless quantities associated with the residual contact stress intensity and the crack geometry, respectively, and P is the indentation load. When $m = 0$, Equation 3 reduces to the case of no crack-resistance toughening. Also $K_r = K_{IC}$ for $m = 0$. It is seen from Equation 3 that the value of m can be evaluated from the best-fit slope of the $\log \sigma_f - \log P$ data shown in Fig. 7. The constant k is evaluated from Equation 2 with the estimated m and the toughness value obtained from the average macroscopic crack size of $c = 1600$ μm from the SEP specimens.

A summary of the fracture parameters m and k thus obtained is shown in Table I. Included in this table is the best-fit slope for each material estimated from the linear regression analysis of $\log \sigma_f$ versus $\log P$. The predicted fracture resistance curve based on Equation 2 is presented in Fig. 8. Neither composite nor monolithic material exhibits any rising R-curve behaviour with a negligibly small toughening exponent of $m \leq 0.04$.

TABLE I Summary of fracture resistance parameters m and k for composite and monolithic materials

Material	Best-fit slope in $\log \sigma_f - \log P$ curve ^a	Fracture resistance parameters	
		m	k
Monolithic	-0.30(0.03)	0.04(0.01)	6.77
Composite	-0.34(0.04)	0	5.18

^a The units are σ_f (MPa) and P (N); also K_r ($\text{MPa m}^{1/2}$) and c (m) in Equation 2. The parentheses indicate ± 1.0 standard deviation.

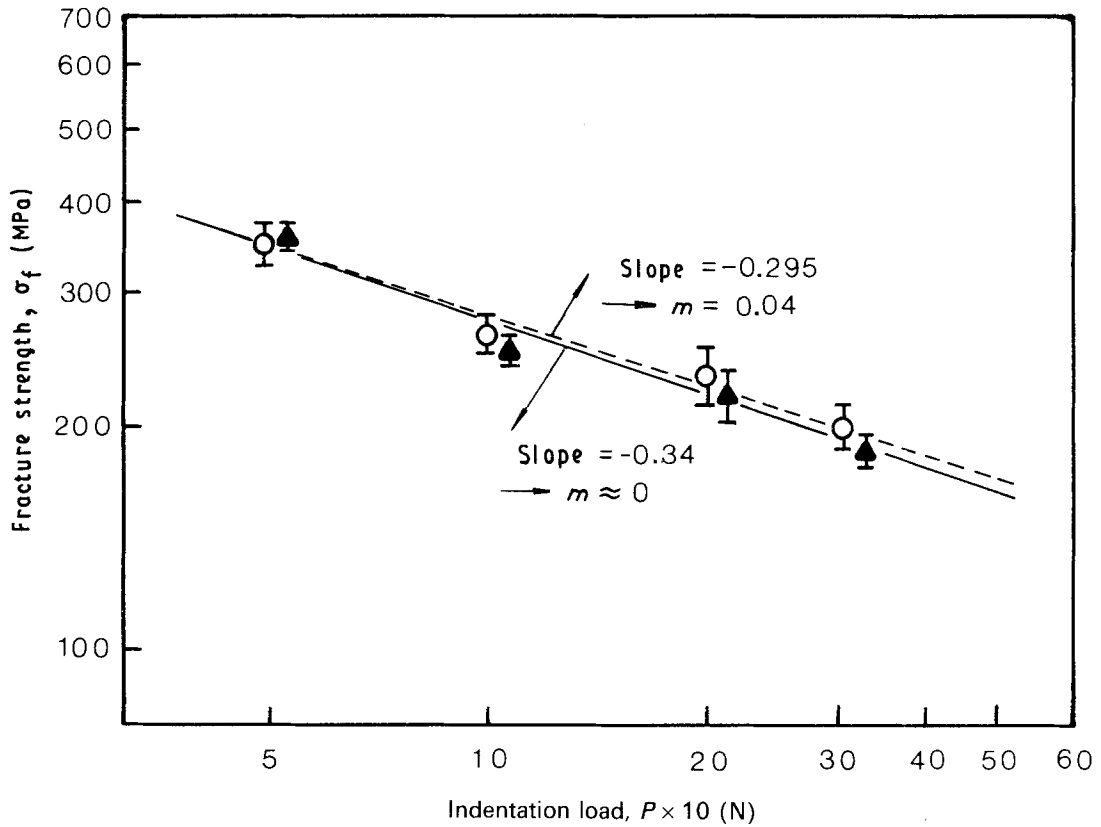


Figure 7 Fracture strength as a function of indentation load for (▲) composite and (○) monolithic materials. Note that the value of m is obtained from the best-fit slope of $\log \sigma_f$ versus $\log P$ curve based on Equation 3. Error bar indicates ± 1.0 standard deviation.

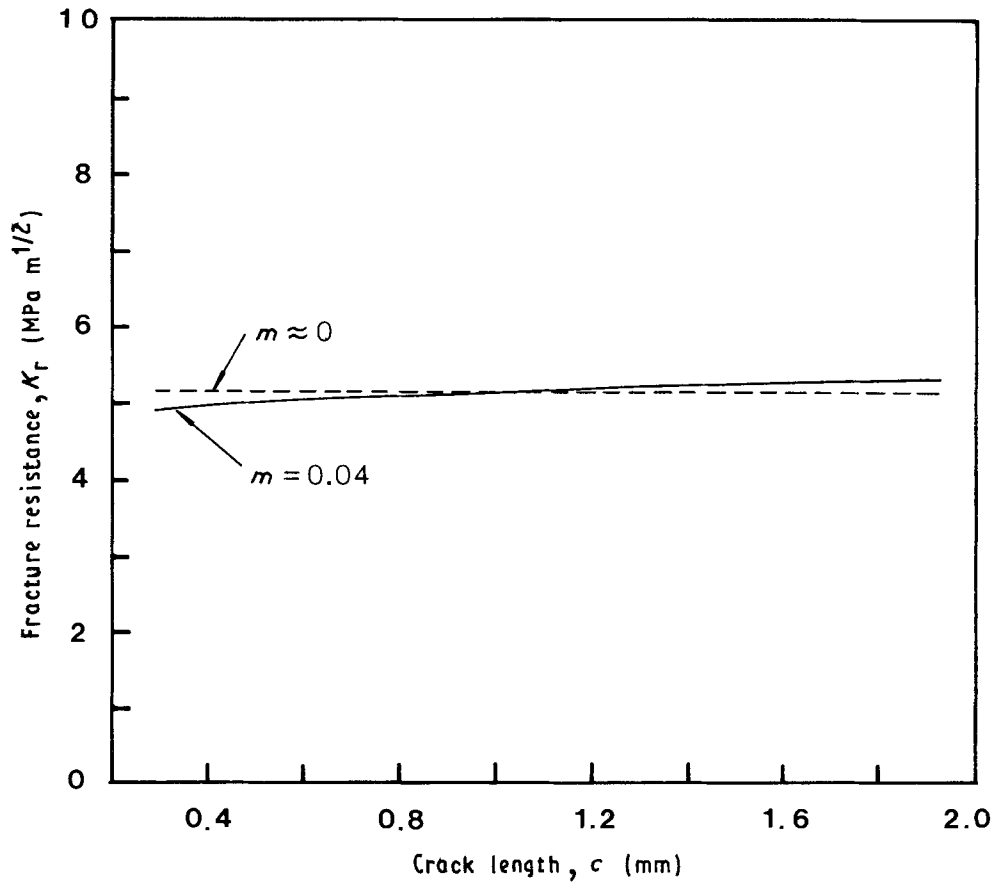


Figure 8 Predicted fracture resistance curves for (---) composite and (—) monolithic materials.

The flat R-curve behaviour for the composite material is also observed from the fracture toughness values evaluated from the SEP specimens at room temperature. Fig. 9 shows a plot of fracture toughness

as a function of normalized crack size a/W , where a is the pre-crack size and W is the specimen height. Here, the different crack sizes were obtained by varying the applied indentation load which not only triggers

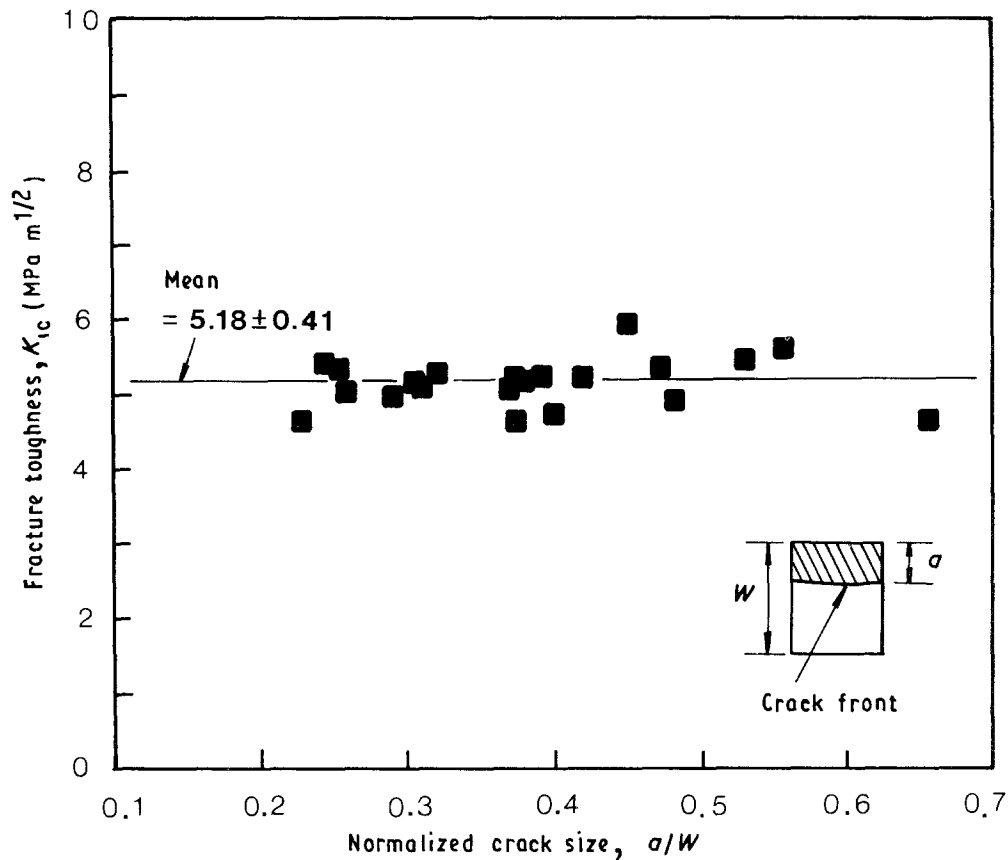


Figure 9 Fracture toughness of composite material as a function of normalized crack size (a/W) measured from the SEPB specimens at 25 °C.

crack pop-in but determines the pre-cracking load and pre-crack size [22]. It can be seen from Fig. 9 that the fracture toughness is insensitive to the crack size, which is consistent with the result obtained from the indentation method (see Fig. 8), since most values are within ± 1.0 standard deviation of the mean ($= 5.18 \text{ MPa m}^{1/2}$).

This result of flat R-curve behaviour for the composite material indicates that whisker addition to the Si_3N_4 matrix did not result in any favourable effect on crack growth resistance. This result is consistent with the previous work on 30 vol % SiC whisker- Si_3N_4 composite material where the toughening exponent was obtained to be $m \leq 0.03$ [26]. Rising R-curve behaviour has been observed with some varying degree for the ceramic materials: Al_2O_3 ($m = 0.13$) [25], 25 wt % SiC whisker-reinforced Al_2O_3 ($m = 0.08$) [29] and *in situ*-toughened Si_3N_4 ($m = 0.1-0.2$) [30, 31].

4. Conclusions

1. No appreciable difference in the as-received strength between the composite and monolithic materials was found at temperatures from 25 to 1400 °C in air. For both materials, strength degradation relative to the room-temperature strength started at about 1200 °C and reached a maximum at 1400 °C. The maximum strength degradation (50 and 45% for the composite and monolithic, respectively) was associated with slow crack growth due to the softening of the grain-boundary glassy phases.

2. Fracture toughnesses of the two materials were almost the same ($5.66 \text{ MPa m}^{1/2}$) and independent of test temperature from 25 to 1200 °C. There was also no distinctive difference in fracture toughness between test methods (chevron-notch, SEPB and indentation strength techniques) at room temperature.

3. Flat R-curve behaviour was observed in both composite and monolithic materials.

4. All of these results indicate that whisker addition to the Si_3N_4 matrix did not provide any favourable effects on strength, fracture toughness and R-curve behaviour.

Acknowledgement

The authors are grateful to R. Pawlik for the experimental and SEM work.

References

1. P. F. BECHER and G. C. WEI, *J. Amer. Ceram. Soc.* **67** (1984) c-267.
2. G. C. WEI and P. F. BECHER, *Amer. Ceram. Soc. Bull.* **64** (1985) 298.
3. J. HOMENY, W. L. VAUGHN and M. K. FERBER, *ibid.* **66** (1987) 333.
4. S. LIO, M. WATANABE, M. MATSUBARA and Y. MATSUO, *J. Amer. Ceram. Soc.* **72** (1989) 188.
5. T. N. TIEGS and P. F. BECHER, *ibid.* **70** (1987) c-109.
6. P. F. BECHER, P. ANGELINI, W. H. WARWICK and T. N. TIEGS, *ibid.* **73** (1990) 91.
7. T. N. TIEGS and P. F. BECHER, in "Tailoring Multiphase and Composite Ceramics", Materials Science Research, Vol. 20 (Plenum, New York, 1986) p. 639.

8. P. F. BECHER, C. H. HSUEH, P. ANGELINI and T. N. TIEGS, *J. Amer. Ceram. Soc.* **71** (1988) 1050.
9. G. H. CAMPBELL, M. RUHLE, B. J. DALGLEISH and A. G. EVANS, *ibid.* **73** (1990) 521.
10. P. D. SHALEK, J. J. PETROVIC, G. F. HURLEY and F. D. GAC, *Amer. Ceram. Soc. Bull.* **65** (1986) 351.
11. S. BULJAN, J. G. BALDONI and M. L. HUCKABEE, *ibid.* **66** (1987) 347.
12. G. PEZZOTTI, I. TANAKA, T. OKAMOTO, M. KOZUMI and Y. MIYAMOTO, *J. Amer. Ceram. Soc.* **72** (1989) c-1461.
13. R. LUNDERBERG, L. KAHLMAN, R. POMPE and R. CARLSSON, *Amer. Ceram. Soc. Bull.* **66** (1987) 330.
14. J. A. SALEM, NASA TM-102423 (National Aeronautics and Space Administration, Lewis Research Center, Cleveland, OH, 1990).
15. J. E. RITTER, S. R. CHOI and K. JAKUS, unpublished work, University of Massachusetts (1989).
16. Y. AKIMUNE, Y. KATANO and K. MATOBA, *J. Amer. Ceram. Soc.* **72** (1989) 791.
17. R. D. NIXON, D. A. KOESTER, S. CHEVACHAROENKUL and R. F. DAVIS, *Compos. Sci. Technol.* **37** (1990) 313.
18. J. G. BALDONI and S. T. BULJAN, in "Ceramic Materials and Components for Engines", Proceedings of 3rd International Symposium, Las Vegas, November 1988 (American Ceramic Society, Westerville, OH, 1989) p. 786.
19. M. BACKHAUS-RICOULT, J. CASTAING and J. L. ROUBORT, *Rev. Phys. Appl.* **23** (1988) 10.
20. S. SURESH, L. X. HAN and J. J. PETROVIC, *J. Amer. Ceram. Soc.* **71** (1988) c-158.
21. D. MUNZ, R. T. BUBSEY and J. L. SHANNON, *ibid.* **63** (1980) 300.
22. T. NOSE and T. FUJII, *ibid.* **71** (1988) 323.
23. P. CHANTIKUL, G. R. ANSTIS, B. R. LAWN and D. B. MARSHALL, *ibid.* **64** (1981) 539.
24. K. F. KRAUSE, *ibid.* **71** (1988) 338.
25. J. E. RITTER, N. BANDYOPADHYAY and K. JAKUS, *Amer. Ceram. Soc. Bull.* **60** (1981) 798.
26. S. R. CHOI and J. SALEM, in "Advanced Composite Materials", Ceramic Transactions, Vol. 19 (American Ceramic Society, Westerville, OH, 1991) p. 741.
27. J. J. PETROVIC, J. V. MILEWSKI, D. L. ROHR and F. D. GAC, *J. Mater. Sci.* **20** (1985) 1167.
28. J. HOMENY, W. L. VAUGHN and M. K. FERBER, *J. Amer. Ceram. Soc.* **73** (1990) 394.
29. R. F. KRAUSE, E. R. FULLER and J. F. RHODES, *ibid.* **73** (1990) 559.
30. J. E. RITTER, S. R. CHOI, K. JAKUS, P. J. WHALEN and R. G. RATEICK, *J. Mater. Sci.* (1991) in press.
31. C. W. LI and Y. YAMANIS, *Ceram. Eng. Sci. Proc.* **10** (1989) 632.

*Received 30 October 1990
and accepted 25 March 1991*